Eur. J. Mineral.
2007, **19**, 463–477
Published online August 2007

Metaluminous pyroxene-bearing granulite xenoliths from the lower continental crust in central Spain: their role in the genesis of Hercynian I-type granites

CARLOS VILLASECA[1,*], DAVID OREJANA[1], BRUCE A. PATERSON[2], KJELL BILLSTROM[3] and CECILIA PÉREZ-SOBA[1]

[1] Departamento de Petrología y Geoquímica, Universidad Complutense, 28040, Madrid, Spain
*Corresponding author, e-mail: granito@geo.ucm.es
[2] Department of Earth Sciences, University of Bristol, BS8 1RJ, Bristol, UK
[3] Swedish Museum of Natural History of Stockholm, Sweden

Abstract: Basic and intermediate meta-igneous xenoliths are very scarce within the granulite population transported by the Permian alkaline lamprophyric dyke swarm of the Spanish Central System (SCS). These xenoliths are metaluminous pyroxene-bearing charnockites (*sensu lato*). They show LREE-poor plagioclase and orthopyroxene-clinopyroxene. Crystallization conditions were estimated at about 850 to 1000 °C and 9 to 11 kbar, a slightly higher range than that estimated for the associated peraluminous granulites, but indicating derivation from the lowermost crust.

Whole-rock geochemistry suggests that the charnockite samples are not a cogenetic suite. The more basic varieties have affinities with cumulates from previous calc-alkaline underplated protoliths, whereas intermediate charnockites have a restitic origin. The similarity in Sr-Nd-Pb isotopic signatures between these restitic charnockites and some SCS I-type granites suggests a genetic relationship. This study, including Pb isotopic data from the whole granulite xenolith suite, reinforces the lower-crustal derivation of the SCS Hercynian granitic batholith.

Key-words: granulite xenoliths, pyroxene mineral chemistry, Hercynian granites, igneous petrology, lower crust, central Spain.

Introduction

The Spanish Central System (SCS) is a moderate-elevation mountain range (1400 m mean elevation) composed mainly of granitic plutons intruded into felsic (meta-granitic and metasedimentary) Palaeozoic and Neoproterozoic continental crust. This large Hercynian batholith is dominated by peraluminous S-type granites, although some minor weakly peraluminous or metaluminous granites of I-type affinity also occur (Villaseca *et al.*, 1998; Bea *et al.*, 1999). The origin of these granites is controversial, concerning the roles of crustal and mantle contribution, especially for I-type granites (*e.g.* Moreno Ventas *et al.*, 1995; Villaseca *et al.*, 1998; Bea *et al.*, 1999).

Upper Permian alkaline lamprophyric dyke swarms cross-cut both granite and basement rocks. They contain abundant deep crustal xenoliths of variable compositions. Studies of lower crustal granulite xenoliths from these alkaline lamprophyres have revitalised the discussion regarding a prevalently crustal origin for the SCS batholith *vs.* involvement of significant mantle-derived magmas. The peraluminous granulite xenolith suite matches the residual composition (major and trace elements, and Sr-Nd-O isotopic ratios) of the outcropping granitic intrusions (Villaseca *et al.*, 1999; Villaseca & Herreros, 2000). This hypothesis is corroborated by geochronological data that show the residual granulites are of Hercynian age, *i.e.* their granulitic imprint was acquired during late-Hercynian times (320 to 285 Ma), identical to the intrusion ages for the SCS plutons (Fernández Suárez *et al.*, 2006). Thus the lower crustal granulite suite of xenoliths seems to represent the residual keel of SCS granites.

In this work we describe pyroxene-bearing mafic and intermediate granulites from the lower crustal xenolith suite that have not been previously studied. These samples comprise around 1 vol.% of the entire xenolith population. We present geochemical data for the whole xenolith suite, trace element microanalysis of major minerals and whole-rock Sr-Nd-Pb isotope ratios and discuss their implications in the genesis of the SCS Hercynian granites.

Geological setting and xenolith petrography

The SCS Hercynian batholith is made by the coalescence of more than a hundred plutons in an age range of around 324 to 285 Ma (Villaseca & Herreros, 2000). Two main granite

DOI: 10.1127/0935-1221/2007/0019-1746
0935-1221/07/0019-1746 $ 6.75
© 2007 E. Schweizerbart'sche Verlagsbuchhandlung, D-70176 Stuttgart

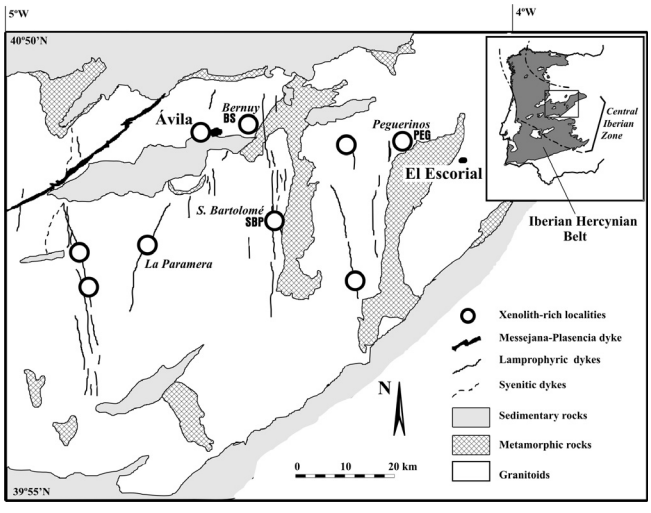

Fig. 1. Geological sketch of the Spanish Central System (SCS) showing the main outcrops where granulite xenoliths are found within the host Permian alkaline lamprophyres and diabases. Localities with complex xenolith population are indicated: BS: Bernuy Salinero, PEG: Peguerinos, SBP: San Bartolomé de Pinares.

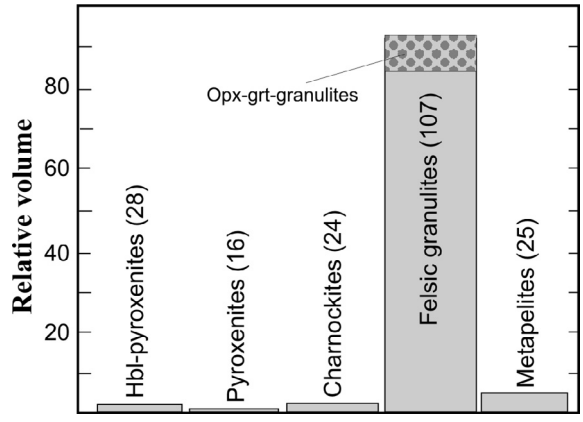

Fig. 2. Lithologic types and abundance of sampled xenoliths (granulites and ultramafic xenoliths) from the SCS alkaline dykes based on their relative abundances. In brackets the number of samples for each group is shown.

types have been distinguished: i) peraluminous cordierite-bearing granites of S-type affinity, and ii) metaluminous to weakly peraluminous biotite-bearing granites with locally accessory amounts of amphibole, described as I-type granites (*e.g.* Villaseca *et al*., 1998). Intermediate granite types without characteristic peraluminous minerals have been also described (*e.g.* Pinarelli & Rottura, 1995). Much debate on SCS granite is related to the relative roles of mantle and crust during their genesis. Some studies suggest a mixed mantle-crustal source for granites (Pinarelli & Rottura, 1995; Moreno-Ventas *et al.*, 1995; Castro *et al.*, 1999) whereas others point to a mainly lower crustal origin (Villaseca *et al.*, 1998, 1999; Bea *et al.*, 1999). The SCS batholith is later intruded by different suites of post-collisional dyke swarms (Villaseca *et al.* 2004): 1) E-W oriented calc-alkaline microdiorites and later shoshonitic microgabbros, all accompanied by abundant coeval granite porphyries, 2) N-S oriented alkaline lamprophyre dykes, and 3) the gabbroic Messejana-Plasencia tholeiitic dyke, the last magmatic event registered in the SCS (dated at 203 Ma, Dunn *et al*., 1998), which has been related to the opening of the Atlantic Ocean. Only the lamprophyre dykes carry deep xenoliths of variable composition.

Lamprophyres have been dated to Upper Permian times (264 to 252 Ma, Perini *et al.*, 2004; Fernández Suárez *et al.*, 2006) and locally were emplaced as diatreme-like, xenolith-rich subvolcanic bodies (Nuez *et al.*, 1982; Villaseca *et al.*, 1999; Bea *et al.*, 1999). The xenolith localities are shown in Fig. 1. The abundance of xenolith types is detailed in Fig. 2 and their general characteristics are described in Table 1. The data presented here double the population of studied xenoliths and enlarge the geographical area sampled, yielding a more representative characterization of the lower continental crust beneath the SCS. The relative abundance of the three main types of granulite xenoliths distinguished by Villaseca *et al.* (1999) is confirmed by this expanded sampling: i) a major population of meta-igneous felsic peraluminous garnet-bearing granulites (approx. 93 vol.% of the total xenolith suite, Fig. 2), including some orthopyroxene-garnet-bearing varieties (Villaseca *et al.*, 1999), ii) metapelites or highly peraluminous garnet-sillimanite-rich granulites (approx. 5 vol.%) of pelitic origin (Villaseca *et al.*, 1999), and iii) charnockites or metaluminous pyroxene-bearing granulites (approx. 1 vol.%). The latter are the main object of this work. Although the SCS xenolith suite consists mainly of granulite crustal xenoliths, there are some minor ultramafic and related mafic xenoliths (pyroxenites and hornblenditic pyroxenites) formed mainly during the alkaline underplating event which gave rise to the lamprophyre dyke swarms (Orejana *et al.*, 2006). The different granulite types coexist in most of the xenolith-rich outcrops, sometimes even in the same thin-section. In three localities (BS, SBP and PEG, Fig. 1), granulite xenoliths are found together with pyroxenitic ultramafic-mafic xenoliths (Orejana *et al.*, 2006).

Pyroxene-bearing granulites may have orthopyroxene, clinopyroxene or both; they form small rounded xenoliths rarely exceeding 5 cm in maximum length. They show a granoblastic texture with no clear evidence of banding likely due to their small size. They are rich in felsic minerals; quartz, K-feldspar and/or plagioclase usually exceeds 50 % in modal amount (Table 1). They plot in the quartz-monzogabbroic (enderbite-jotunite) to gabbroic (norite) modal fields (Fig. 3). Although the marked dominance of plagioclase among felsic minerals prevents their classification as charnockites s.s., this name will be used informally through the text to refer to these metaluminous pyroxene-bearing xenoliths.

SCS charnockite mineralogy comprises plagioclase, quartz, K-feldspar, orthopyroxene and clinopyroxene as major phases. Peraluminous minerals (sillimanite, garnet, Al-phlogopite) are lacking, in contrast with the other two coexisting groups of lower crustal granulite xenoliths (Villaseca *et al.* 1999). Accessory phases include rutile, sphene, apatite, ilmenite, zircon and pyrrhotite.

Table 1. Xenolith types in the Permian SCS alkaline lamprophyres.

Sample	Mineralogy (modal amount in vol.%)	Texture	Size	(Composition) Nature
	Hornblenditic pyroxenites			*Ultrabasic-Basic*
103489	amph (40), cpx (40), pl (13), ap (3), spl (2), anl (2), cc	igneous	1–2 cm	Alkaline ultramafic cumulate (Orejana *et al.*, 2006)
104389	cpx (69), amph (15), pl (10), phl (3), anl (1), ap, spl, cc	igneous	0.5–1.5 cm	"
	Pyroxenites s.l.			*Ultrabasic-Basic*
101892	*Clinopyroxenite:* cpx (94), spl (6)	cataclastic	< 0.5 cm	Alkaline? ultramafic cumulate (Orejana *et al.*, 2006)
102131	*Websterite:* cpx (57), opx (42), spl (1)	granoblastic	< 0.5 cm	calc-alkaline ultramafic cumulate (Orejana *et al.*, 2006)
104395	*Pyroxenite*: cpx (77), chl (opx?) (19), spl (2), cc	granoblastic	< 0.5 cm	"
	Charnockites s.l. *(Type 1 of VDPB-99)*			*Basic-intermediate, metaluminous (meta-igneous rocks)*
103490B	pl (83), opx (16), ilm (1), zrn, ap	granoblastic	1 cm	residual granulite (this work)
105775	pl (58), cpx (23), opx?(12), rt (2), ap	granoblastic	1.5 cm	calc-alkaline cumulate (this work)
105779	pl (80), cpx (16), ilm (2), ap, zrn, spn, cc	granoblastic	1 cm	residual granulite (this work)
U-28	pl (64), opx (29), cpx (5), rt, ap, zrn, ilm	granoblastic	1 cm	"
U-3	pl (54), qtz (17), kfs (17), opx (10), ap (1), zrn, ilm	granoblastic	2.5 cm	"
	Felsic granulites *(Type 2 of VDPB-99)*			
	Opx-grt-granulites (Type 2a)			*Intermediate-acid, peraluminous (meta-igneous rocks)*
103184	pl (53), grt (28), opx (18), ilm (1), qtz, ap, zrn	granoblastic, banded	1–5 cm	residual granulite (Villaseca *et al.*, 1999)
81845	kfs (47), pl (32), grt (10), opx (5), qtz (3), rt, ap, zrn, ilm	granoblastic	2–3 cm	"
105796	pl (40), qtz (33), grt (22), opx (3), ilm (1), phl, ap, zrn	granoblastic, banded	2–3 cm	"
	Felsic granulites ss (Type 2b)			*Intermediate-acid, peraluminous (meta-igneous rocks)*
U-50	grt (40), kfs (32), pl (19), qtz (3), phl (1), rt (1), ap, zrn	granoblastic, banded	10 cm	residual granulite (Villaseca *et al.,*1999)
95141	kfs (55), qtz (24), grt (17), sil (3), rt (1), pl, ap, zrn	granoblastic, banded	8–12 cm	"
99185	qtz (37), pl* (34), grt (28), rt (1), ap, zrn, mnz	granoblastic, banded	6 cm	"
	Metapelitic granulites *(Type 3 of VDPB-99)*			*Highly peraluminous (meta-sedimentary rocks)*
77750	kfs (45), grt (22), qtz (18), sil (13), rt (1), ap, zrn, mnz	granoblastic, banded	7–10 cm	residual granulite (Villaseca *et al.,*1999)
U-90	grt (38), pl (29), kfs (16), sil (11), rt (2), qtz (1), ap	granoblastic	6 cm	"
104550	grt (71), sil (25), pl (3), rt (1), ilm, zrn	granoblastic	4 cm	highly restitic granulite

VDPB-99 = Villaseca *et al.* (1999). Mineral abbreviations after Kretz (1983) except: amph = amphibole, pl* = ternary feldspar. Modal analyses of pyroxenite xenoliths from (Orejana *et al.*, 2006), felsic and metapelitic granulites from (Villaseca *et al.*, 1999).

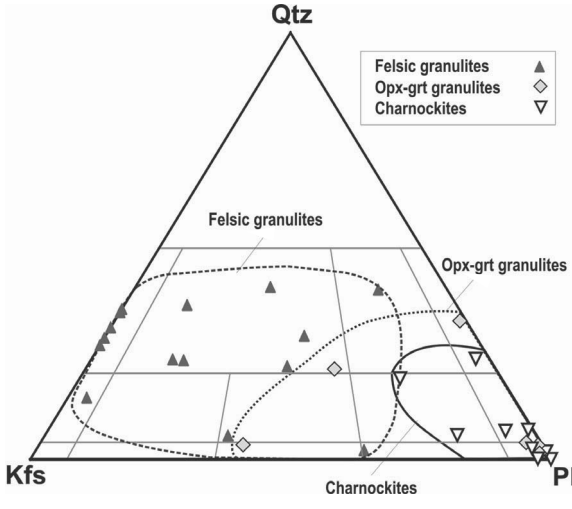

Fig. 3. Modal composition of the SCS granulite xenoliths in terms of Kfs-Qtz-Pl proportions.

The peraluminous orthopyroxene-garnet-(phlogopite)-bearing granulites (type 2a from Villaseca *et al.*, 1999) (Table 1) are more felsic in modal composition than the metaluminous charnockites (Fig. 3), and show different mineral and whole-rock chemical compositions, as it will be exposed below.

Analytical methods

Major element mineral composition was determined at the *Centro de Microscopía Electrónica "Luis Bru" (Complutense University of Madrid)* using a JEOL JZA-8900M electron microprobe (EMP) with four wavelength dispersive spectrometers. Analyses were performed with an accelerating voltage of 15 kV and an electron beam current of 20 nA, with a beam diameter of 2–5 μm. Elements were counted for 10 s on the peak and 5 s on each of two background positions. Corrections were made using the ZAF method.

Concentrations of 24 trace elements (REE, Ba, Rb, Th, U, Nb, Ta, Sr, Zr, Hf and Y) were determined on major mineral phases on > 130 μm thick polished sections by laser ablation ICP-MS (LA-ICP-MS) at the *Department of Earth Sciences* (University of Bristol) using a VG LaserProbe II (266 nm frequency-quadrupled Nd-YAG laser) coupled to a VG Elemental PlasmaQuad 3 ICP-MS. The diameter of the laser spots was approximately 20–30 μm. The counting time for each analysis was typically 100 s (40 s measuring gas blank to establish the background and 60 s for the remainder of the analysis). The NIST 610 and 612 glass standards were used to calibrate relative element sensitivities for the analyses of the silicate minerals. Each laser analysis used Si (for feldspars and orthopyroxene) and Ca (for clinopyroxenes) as an internal standard, with concentrations determined by electron microprobe. Ti was the internal standard for rutile analyses.

Table 2. Selected representative EMP analyses of feldspars from the SCS charnockite xenoliths.

Sample	102142	U-3	U-3	102131	104390B	104551	104867	105775	105775	U-28	U-28	U-3
Analysis	40	68	70	4	49	5	67	60	12	24	15	61
Mineral	Kfs	Kfs	Kfs	Plg	Plg	Plg	Plg	Plg	Plg	Plg	Plg	Plg
SiO_2	64.13	64.17	63.30	53.28	58.28	53.24	59.45	49.28	50.98	56.19	57.98	57.20
TiO_2	0.03	0.07	0.00	0.06	0.04	0.03	0.01	0.08	0.08	0.02	0.01	0.01
$Al2O_3$	20.12	18.97	19.12	29.77	25.68	28.92	25.25	30.87	30.34	26.91	25.76	26.11
FeO	0.01	0.11	0.00	0.09	0.09	0.21	0.18	0.23	0.28	0.15	0.16	0.10
MnO	0.00	0.00	0.00	0.05	0.01	0.04	0.02	0.02	0.04	0.02	0.01	0.00
MgO	0.00	0.00	0.03	0.06	0.02	0.05	0.03	0.10	0.08	0.04	0.04	0.00
CaO	1.03	0.78	0.26	12.10	7.75	12.51	7.76	14.60	14.86	8.88	9.11	8.84
Na_2O	4.90	3.52	0.71	4.38	6.52	3.73	6.70	3.23	2.51	5.83	5.42	6.99
K_2O	8.51	12.28	15.41	0.43	1.02	0.93	1.03	0.27	0.28	1.15	1.21	1.47
P_2O_5	0.00	0.06	0.01	0.02	0.05	0.02	0.02	n.d.	0.04	n.d.	0.01	0.05
Total	98.72	99.96	98.83	100.69	99.99	99.98	100.90	98.67	99.47	99.18	99.71	100.77
Si	11.666	11.781	11.778	9.618	10.490	9.693	10.597	9.138	9.337	10.212	10.450	10.305
Al	4.310	4.102	4.256	6.329	5.444	6.200	5.301	6.741	6.543	5.758	5.468	5.511
Ti	0.005	0.010	0.000	0.008	0.005	0.004	0.001	0.012	0.010	0.003	0.001	0.002
Fe_2	0.001	0.016	0.000	0.014	0.014	0.032	0.027	0.036	0.042	0.022	0.024	0.014
Mn	0.000	0.000	0.000	0.008	0.002	0.006	0.003	0.003	0.006	0.002	0.002	0.000
Mg	0.000	0.000	0.008	0.016	0.005	0.014	0.008	0.027	0.022	0.010	0.012	0.000
Ca	0.201	0.154	0.053	2.340	1.495	2.440	1.482	2.901	2.916	1.730	1.760	1.697
Na	1.729	1.254	0.262	1.533	2.276	1.317	2.316	1.161	0.890	2.053	1.895	2.430
K	1.975	2.875	3.717	0.099	0.234	0.216	0.234	0.063	0.066	0.267	0.277	0.335
P	0.000	0.010	0.000	0.000	0.010	0.000	0.000	-	0.010	-	0.000	0.010
Cations	19.887	20.202	20.074	19.965	19.975	19.922	19.969	20.082	19.842	20.057	19.889	20.304
Ab	44.30	29.30	6.50	38.60	56.80	33.10	57.40	28.10	23.00	50.70	48.20	54.50
An	5.10	3.60	1.30	58.90	37.30	61.40	36.80	70.30	75.30	42.70	44.80	38.00
Or	50.60	67.10	92.20	2.50	5.80	5.40	5.80	1.50	1.70	6.60	7.00	7.50

Whole-rock major and trace element analyses of seven xenoliths (4 charnockites and 3 opx-grt-granulites) were determined at the CNRS-CRPG, Nancy. The samples were fused using $LiBO_2$ and dissolved with HNO_3. Solutions were analysed by inductively coupled plasma atomic emission spectrometry (ICP-AES) for major elements, whilst trace elements were determined by ICP mass spectrometry (ICP-MS). Uncertainties in major elements are generally between 1 and 3 %, except for MnO (5–10 %) and P_2O_5 (> 10 %), whereas most of the trace elements have uncertainties <10 %. More information on the procedure, precision and accuracy of Nancy ICP-MS analyses is given by Carignan *et al.* (2001).

The same xenoliths were also selected for combined Sr-Nd isotopic analyses at the *CAI de Geocronología y Geoquímica Isotópica* of the Complutense University of Madrid, using an automated VG Sector 54 multicollector thermal ionisation mass spectrometer with data acquired in multidynamic mode. Isotopic ratios of Sr and Nd were measured on an aliquot of whole-rock powder. The Sr-Nd analytical procedures used in this laboratory have been described elsewhere (Reyes *et al*., 1997). Repeated analysis of NBS 987 gave $^{87}Sr/^{86}Sr = 0.710249 \pm 30$ ($2\sigma, n = 15$) and for the JM Nd standard the $^{143}Nd/^{144}Nd = 0.511809 \pm 20$ ($2\sigma, n = 13$). The 2σ error on calculated ε(Nd) values is ±0.4.

Two charnockites, one opx-grt granulite and five other peraluminous granulite xenoliths were selected for Pb isotopic analyses at the Natural History Museum of Stockholm University using a Finnigan MAT 261 TIMS with multicollector and a secondary electron multiplier. It was only possible to prepare K-feldspar separates from three of the peraluminous granulite xenoliths (Table 7). The Pb isotope composition of the two pyroxenite xenoliths of probable calc-alkaline affinity from Orejana *et al*. (2006) have been also studied for comparison. The samples were dissolved with HF and HNO_3. A ^{205}Pb spike was added to each sample. Pb was separated using cation exchange columns. The NBS 981 and 982 elemental Pb standards were used to evaluate fractionation and precision, the latter being around 0.1 % for the isotopic ratios shown in Table 7. Repeated analyses of international standard BCR-1 were used to monitor accuracy.

Mineral chemistry

Feldspars

Representative EMP analyses of charnockite feldspars are shown in Table 2. K-feldspar always represents < 20 vol.% of the xenolith (Table 1). K-feldspar has a greater Or component in interstitial areas and in rims (Or_{95}) than in inner zones ($Or_{50–70}$). Although their major element composition resembles that of feldspars from the SCS peraluminous granulite xenoliths, their P_2O_5 content is significantly lower, always < 0.06 wt.%, and at least three times lower than feldspars in coexisting peraluminous types (Fig. 4b).

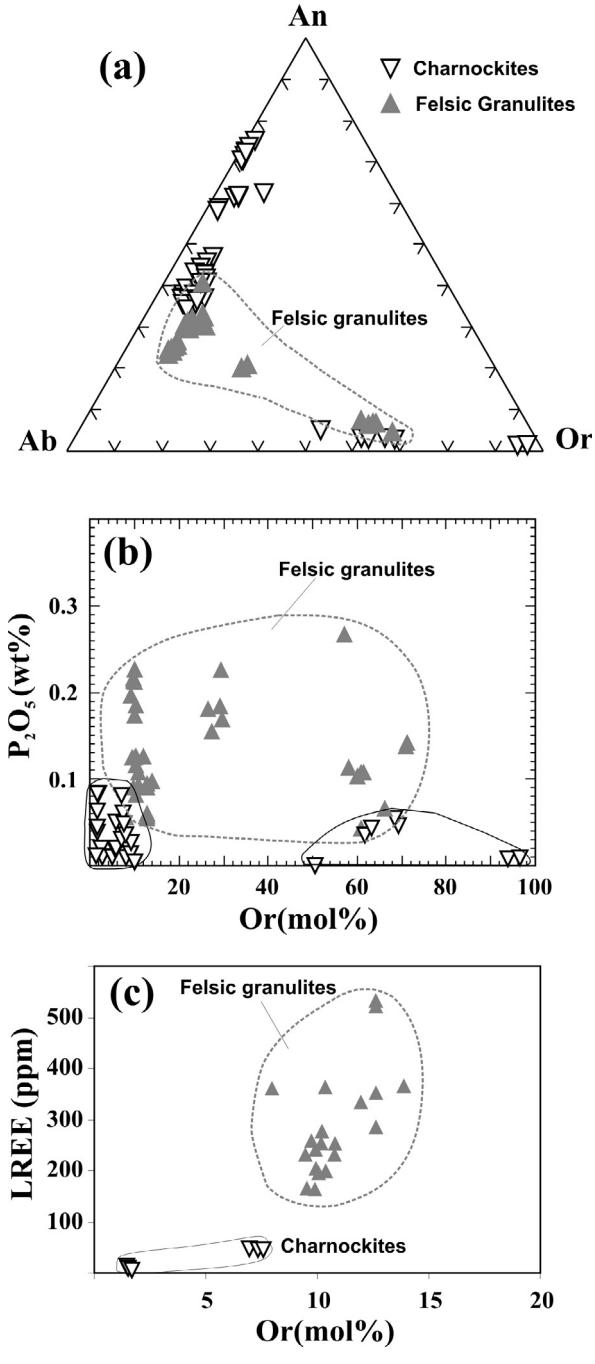

Fig. 4. Feldspar composition of SCS granulite xenoliths: a) Ternary Ab-An-Or diagram; b) Or *vs.* P_2O_5; c) Or *vs.* total LREE contents.

Plagioclase is the most abundant mineral in the charnockites, ranging from 50 to 75 vol.% of the xenolith. Its composition varies between An_{37} to An_{73}, being more Ca-rich than plagioclase from peraluminous xenoliths. Plagioclase in the charnockites is also lower in K_2O (Or < 10 mol%) and P_2O_5 (< 0.1 wt.%) contents (Fig. 4) compared to the peraluminous xenoliths.

Major differences are apparent when the trace element contents of feldspars are considered. Plagioclase in the charnockites have low LREE contents, in the range of 7–50 ppm (Table 2), as is common in metaluminous granulites (Pride & Muecke, 1981; Loock *et al.*, 1990), whereas plagioclases in SCS peraluminous granulites show much higher LREE contents, in the range of 150–550 ppm (Villaseca *et al.*, 2003) (Fig. 4c). Other lower crustal granulite xenoliths of peraluminous composition also have LREE-rich plagioclases (Reid, 1990; Condie *et al.*, 2004), similarly to those of SCS felsic meta-igneous xenoliths (Villaseca *et al.*, 2007). Charnockite plagioclase also shows slightly lower Rb-Ba-(Sr) contents than plagioclase from peraluminous granulites.

Pyroxenes

SCS pyroxene-bearing granulites typically contain 10–40 vol.% orthopyroxene, clinopyroxene or both, always subordinate to modal plagioclase (Table 1). Pyroxene is the only mafic phase in these xenoliths. Pyroxenes are chemically varied suggesting that the granulites are compositionally heterogeneous; orthopyroxene ranges from En_{76} to En_{43} and is richer in Wo (1–3 %) than orthopyroxenes from peraluminous opx-grt-granulites. In contrast, orthopyroxenes from these peraluminous granulites have a more restricted compositional range (En_{61} to En_{45}, Table 3). The high CaO (0.5 to 1.2 wt.%) and low Al_2O_3 contents (1.4 to 6 wt.%) of charnockite orthopyroxenes distinguish them from peraluminous granulite orthopyroxenes (Fig. 5a).

Clinopyroxene only appears in charnockites within the SCS xenolith suite. XMg in clinopyroxene varies from 0.80 to 0.68 with variable CaO (18.4 to 24.6 wt.%) and Al_2O_3 (mostly from 1.6 to 4.3 wt.%) contents (Fig. 5b). In one granulite, that is located in the same sample (102131) of the only websterite xenolith found in the SCS lamprophyres (Orejana *et al.*, 2006), clinopyroxene shows high Na_2O (up to 1.1 wt.%) and Al_2O_3 (up to 8.3 wt.%) contents, equivalent to 8.2 mol% jadeite. In all cases, bar the previously mentioned granulite 102131, granulitic clinopyroxenes show lower TiO_2, Cr_2O_3, NiO, Na_2O and Al_2O_3 contents when compared to clinopyroxene from SCS ultramafic xenoliths (Fig. 5b).

Orthopyroxene shows much lower trace element concentrations than clinopyroxene. Orthopyroxene in SCS metaluminous granulites show higher Sc, Cr, Y, and HREE contents than those from garnet-bearing peraluminous types; however the latter are notably richer in V (Table 4). Moreover, their chondrite-normalized REE patterns display a marked positive HREE fractionation (Gd_N/Er_N = 0.3) whereas orthopyroxene from peraluminous opx-grt granulites show a negative HREE fractionation (Gd_N/Er_N = 3.5) (Fig. 6a). There are also remarkably similar trace element composition and REE patterns in the orthopyroxenes from the two-pyroxene granulite and the websterite (Fig. 6a), both from the same sample 102131.

Clinopyroxene shows a more variable trace element composition. In sample 105775 clinopyroxene has higher Y-HREE contents than clinopyroxene from ultramafic pyroxenites (Fig. 6b). The charnockite clinopyroxene has lower LILE (Rb, Sr, Ba), HFSE (Nb, Th, Zr, Hf, Ta) and LREE contents than clinopyroxene from SCS ultramafic xeno-

Table 3. Selected representative EMP analyses of pyroxenes from the SCS charnockite xenoliths.

Sample	105796*	103490B	104867	U-3	102131	U28	U28	102131	102142	104551	105775	105779
Analysis	52	32	73	54	6	18	17	5	42	7	52	80
Mineral	Opx	Opx	Opx	Opx	Opx	Opx	Cpx	Cpx	Cpx	Cpx	Cpx	Cpx
SiO2	48.73	49.75	50.18	50.72	52.22	52.34	51.40	49.47	51.54	52.30	49.91	51.01
TiO2	0.28	0.23	0.13	0.27	0.54	0.17	0.44	0.64	0.11	0.66	1.17	0.58
Al2O3	6.09	4.19	1.86	2.40	5.85	1.43	2.39	8.33	1.75	3.33	4.30	2.65
FeO	22.13	23.99	32.44	27.98	13.82	18.98	8.05	6.13	11.35	8.44	9.95	10.59
Cr2O3	0.10	0.09	-	0.01	-	-	-	0.03	0.05	0.25	0.22	0.05
MnO	-	0.37	0.70	0.53	0.26	0.34	0.14	0.13	0.20	0.15	0.27	0.83
MgO	21.27	19.58	14.45	17.22	26.41	24.51	14.96	13.57	10.70	14.73	14.27	12.73
CaO	0.21	0.57	0.50	0.89	0.90	1.05	21.03	20.20	24.63	20.15	18.51	20.64
Na2O	-	0.02	0.03	0.03	0.11	0.01	0.47	1.08	0.27	0.34	0.24	0.24
K2O	0.01	0.01	-	0.02	-	-	-	0.01	-	-	-	-
Total	98.82	98.80	100.29	100.07	100.11	98.83	98.87	99.59	100.60	100.35	98.81	99.32
TSi	1.828	1.892	1.962	1.945	1.866	1.939	1.919	1.815	1.940	1.932	1.881	1.930
TAl	0.172	0.108	0.038	0.055	0.134	0.061	0.081	0.185	0.060	0.068	0.119	0.070
M1Al	0.097	0.080	0.047	0.053	0.113	0.001	0.024	0.175	0.018	0.076	0.071	0.048
M1Ti	0.008	0.007	0.004	0.008	0.015	0.005	0.012	0.018	0.003	0.018	0.033	0.016
M1Fe2	0.000	0.000	0.107	0.000	0.000	0.000	0.131	0.064	0.357	0.087	0.087	0.216
M1Cr	0.003	0.003	0.000	0.000	0.000	0.000	0.000	0.001	0.001	0.007	0.007	0.001
M1Mg	0.892	0.911	0.842	0.938	0.870	0.994	0.832	0.742	0.601	0.811	0.802	0.718
M2Mg	0.297	0.200	0.000	0.046	0.537	0.359	0.000	0.000	0.000	0.000	0.000	0.000
M2Fe2	0.694	0.763	0.954	0.897	0.413	0.588	0.120	0.124	0.000	0.174	0.226	0.119
M2Mn	0.000	0.012	0.023	0.017	0.008	0.011	0.004	0.004	0.006	0.005	0.008	0.027
M2Ca	0.009	0.023	0.021	0.037	0.034	0.042	0.841	0.794	0.993	0.797	0.747	0.837
M2Na	0.000	0.001	0.002	0.002	0.008	0.001	0.034	0.077	0.020	0.024	0.018	0.018
M2K	0.000	0.000	0.000	0.001	0.000	0.000	0.000	0.000	0.000	0.000	0.000	0.000
Cations	4.000	4.000	4.000	3.999	4.000	4.000	4.000	4.000	4.000	4.000	4.000	4.000
WO	0.45	1.22	1.08	1.89	1.85	2.09	43.61	45.94	50.75	42.55	39.95	43.67
EN	62.86	58.17	43.26	50.86	75.55	67.88	43.14	42.94	30.67	43.28	42.85	37.46
FS	36.69	40.61	55.67	47.26	22.60	30.03	13.25	11.12	18.58	14.16	17.21	18.87

* Peraluminous orthopyroxene-bearing SCS felsic xenolith.

liths. Some clinopyroxenes show convex-upward LREE patterns with a peak at Sm, similar to the general pattern of clinopyroxene in ultramafic xenoliths with the exception of marked negative Eu anomalies (Fig. 6). Clinopyroxene from charnockite 102131 has a flatter REE pattern and a marked positive Eu anomaly. Clinopyroxene showing negative Eu anomalies are common in mafic granulite xenoliths (Loock *et al.*, 1990; Upton *et al.*, 2001; Storkey *et al.*, 2005), whereas those with positive anomalies are more unusual and have been interpreted as indicative of high oxygen fugacity during high-T metamorphism (Rogers & Hawkesworth, 1982; Loock *et al.*, 1990) or by metamorphic reaction with feldspar in plagioclase-rich granulites (Ulianov *et al.*, 2006).

Accessories

Charnockite rutile has high Zr contents (close to 4500 ppm), slightly lower than in associated peraluminous granulites, where they can reach 6900 ppm (Villaseca *et al.*, 2007). The high Zr content of charnockite rutiles is typical of granulite-facies conditions (Zack *et al.*, 2004). Apatites have high total LREE contents (around 7300 ppm) and significant amounts of Sr (300 ppm) and Th (32 ppm) (Table 4). They have high Ce_N/Yb_N ratios (15) and low Eu/Eu* values (0.13), the latter being much lower than in other mafic granulites (Loock *et al.*, 1990; Upton *et al.*, 2001), and typical of equilibration with the modally abundant plagioclase (Storkey *et al.*, 2005).

P-T estimates

Equilibration pressures of the charnockite xenoliths must have been less than 10–12 kbar, otherwise garnet would have been stable. In melting experiments on tonalite rocks, garnet replaces orthopyroxene at pressures > 12 kbar (Patiño Douce & McCarthy, 1998) and garnet also appears at 10 kbar in most meta-gabbro melting experiments (*e.g.* Springer & Seck, 1997). P-T estimates were obtained using the PTMAFIC program of Soto & Soto (1995). Pressures of between 9 to 12 kbar were obtained using cpx + plag + qtz equilibria (Ellis, 1980) in those charnockites with two pyroxenes or only clinopyroxene (Table 5). Pressure estimates based on garnet-orthopyroxene equilibria (Newton & Perkins, 1982; Brey *et al.*, 1986) for associated peraluminous granulite xenoliths gave similar values mostly in the range of 9 to 11 kbar (Table 5). Moreover, SCS pyrox-

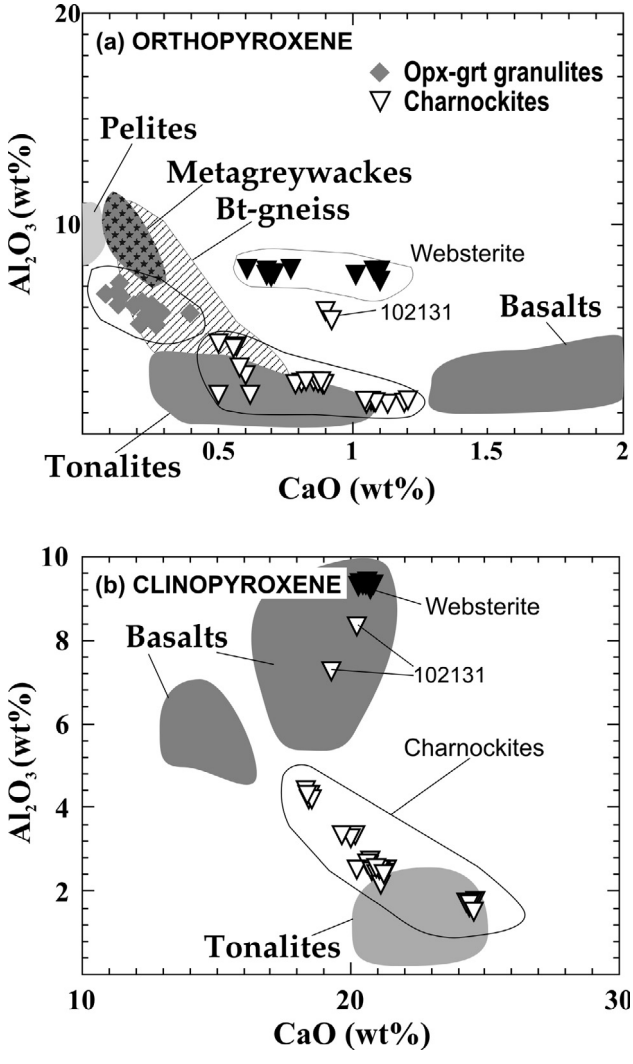

Fig. 5. CaO *vs.* Al_2O_3 (wt.%) in pyroxene from various SCS granulite xenoliths: a) orthopyroxene, b) clinopyroxene. Websterite pyroxene compositional field is taken from Orejana *et al.* (2006). Pyroxene from SCS granulite xenoliths are compared to compositional fields of restitic pyroxenes in melting experiments (at conditions of vapor-absent and P of 5 to 12 kbar). Fields are average pyroxene composition from partial fusion experiments of pelites (Carrington & Harley, 1995), aluminous metagreywackes (Montel & Vielzeuf, 1997), biotite gneisses (Patiño Douce & Beard, 1995), tonalites (Singh & Johannes, 1996), and basalts (meta-gabbro 87S35A from Sisson *et al.* 2005; metabasites from Springer & Seck, 1997).

Table 4. Average mineral trace element (LA-ICPMS) composition (in ppm).

Mineral	**Pl**	**Pl**	**Opx**	**Opx**	**Opx**	**Cpx**	**Cpx**	**Rt**	**Ap**
Sample	105775	U-28	U-28	102131	105796*	102131	105775	U-28	U-28
n	3	3	3	2	3	1	4	2	2
Li	24.83	1.78							2.21
P	177	142						114	133900
Sc	3.04	2.58	43.37		24.94		115	29.33	2.62
V	3.20	1.06	293	292	772	182	527	2285	4.34
Cr	17.09	11.74	986	98.29	377	69.39	1336	4824	9.29
Rb	120	4.25				0.56			
Sr	451	498	0.43			51.65	19.03		303
Ba	304	270							7.69
Zr			5.40	7.32	13.87	6.69	65.78	4433	4.27
Nb						1.06		1255	
Ta						0.06		51.61	
Hf			0.25	0.46	0.91	0.29	2.77	103	0.12
Pb	1.05	14.40	0.16				0.24	0.40	5.17
Th						0.72	0.20		31.92
U								7.40	4.82
Y	0.54	0.56	12.42	2.20	3.19	3.27	47.97	1.01	1035
La	2.00	14.99				1.84	3.09		1279
Ce	4.53	23.84	0.29	0.05	0.31	5.47	11.68		3263
Pr	0.52	2.12			0.10	0.73	2.61		434
Nd	2.17	6.40	0.82		1.09	2.52	17.92		1970
Sm	0.55	0.74	0.63		1.00	1.14	8.12		403
Eu	1.00	1.93				1.08	0.51		14.35
Gd			0.65		1.24	0.77	8.98		321
Tb			0.22	0.10	0.17	0.13	1.57		42.76
Dy		0.29	1.83	0.31	0.91	0.63	9.76		216.4
Ho			0.49	0.11	0.17	0.17	1.99		39.48
Er			1.63	0.35	0.49	0.53	5.05		89.94
Tm		0.05	0.34	0.07		0.10	0.69		10.30
Yb			2.68	0.39		0.43	4.26		56.04
Lu			0.51	0.10		0.13	0.60		6.90

Blank rows mean below detection limits by LA-ICPMS.
* Peraluminous orthopyroxene-garnet-bearing xenolith.

enite xenoliths yielded the same pressure range for recrystallization (Orejana *et al.*, 2006).

Temperatures estimates in charnockites have been determined using two-pyroxene or Ca-in-orthopyroxene geothermometers (Wells, 1977; Wood & Banno, 1973; Brey & Köller, 1990). A range of 915 to 1060°C has been obtained (Table 5). The garnet-orthopyroxene geothermometer of Harley (1984) and Al-in-orthopyroxene equilibria of Witt-Eickschen & Seck (1991) give similar values of 870 to 990 °C for the more felsic peraluminous orthopyroxene-garnet granulites. Moreover, the occurrence of orthopyroxene in peraluminous granulites with high-Ti-F mica and a Ti-bearing phase (rutile/ilmenite) has been observed experimentally in the range 925 to 1050 °C for the estimated pressure conditions (Nair & Chacko, 2002).

Estimated temperatures in SCS pyroxene-bearing xenoliths are slightly higher than those for the felsic granulite xenoliths, a situation that occurs in other xenolith suites; pyroxene thermometry tends to overestimate temperature (*e.g.* Al-Mishwat and Nasir, 2004). Similarly, the application of Zr-in-rutile geothermometry yields a varied range of T estimates, depending of the calibration used. The empirical version of Zack *et al.* (2004) gives 960 to 1060 °C, whilst the experimental approach of Watson *et al.* (2006) yields a range of 830 to 930 °C (Table 5).

These results overlap with the estimated granulitic $P - T$ conditions in the SCS felsic and pelitic xenolith suites (Villaseca *et al.*, 1999), although $P - T$ estimates in the charnockites are higher. Nevertheless, estimated equilibration pressures, mostly in the range of 9 to 11 kbar, suggest that all quartz-feldspathic xenoliths could be derived from lower crustal levels. In addition, these $P - T$ estimates are in agreement with the lack of garnet in basic granulites and the general presence of sillimanite (instead of kyanite) in associated peraluminous granulite xenoliths.

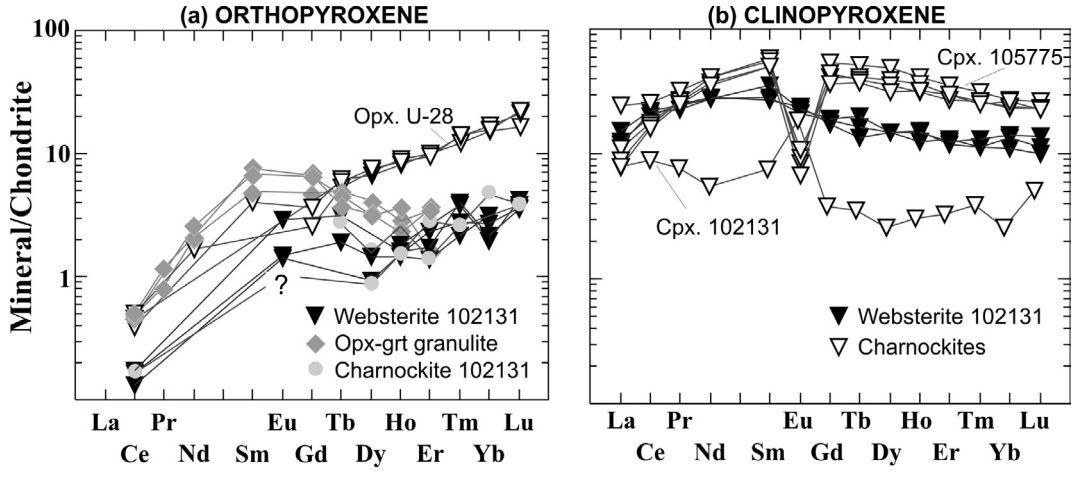

Fig. 6. Chondrite-normalised REE patterns for pyroxenes from SCS granulite xenoliths: a) orthopyroxene, b) clinopyroxene. Normalising values are from Sun & McDonough (1989). Pyroxene websterite data (inverted full triangle) are from Orejana *et al.* (2006). Orthopyroxene from charnockite 102131 (full circle) plot above websterite data.

Table 5. $P - T$ determinations on SCS pyroxene-bearing xenoliths.

	Xenolith type	T(1)	T(2)	T(3)	T(4)	T(5)	T(6)	P(1)	P(2)	P(3)
102131	Charnock. 2 pyrox.	1017	988		1006					
U-28	"	935	958		1062	918	988	12		
104551	Charnock. Cpx					930	1060	9-12.7		
105775	"					827	960	10		
104867	Charnock. Opx				943					
103490B	"				916					
U-3	"				1023					
105796	(Opx-Grt) Felsic			950	973	740	850		12.7	11
81846	"			870	992				9.2	
81845	"			910	894				11.0	9.4

T in °C and P in kbar. T(1) Wood & Banno (1973); T(2) Wells (1984); T(3) Harley (1984); T(4) Brey & Koler (1990) for charnockites, and Witt-Eickschen & Seck (1991) for orthopyroxene-bearing felsic granulites; T(5) Watson *et al.* (2006); T(6) Zack *et al.* (2004); P(1) Ellis (1980); P(2) Newton & Perkins (1982); P(3) Brey *et al.* (1986).

Whole-rock geochemistry

Major elements

Major and trace element data for 7 whole-rock samples (4 charnockites and 3 orthopyroxene-garnet granulites) are given in Table 6.

Although charnockites are aluminium-rich (with 14 to 19 wt.% Al_2O_3) they are always metaluminous in composition, in contrast with orthopyroxene-garnet granulites which are moderately to highly peraluminous (A/CNK values from 1.2 to 1.7). According to their SiO_2 content, charnockites range from basic to mainly intermediate composition whereas orthopyroxene-garnet granulites are more silica-rich (intermediate to acid) (Table 6). Charnockites show lower Al_2O_3, FeO, TiO_2, K_2O and higher CaO contents than felsic and pelitic xenoliths (Fig. 7). Nevertheless, they show a high K_2O content, mainly from 1.65 to 3.38 wt.%, plotting mostly in high-K fields on the basis of their concentrations of K_2O and SiO_2 (Le Maitre *et al.*, 1989). MgO and Na_2O contents are intermediate between those of felsic and pelitic xenoliths (Fig. 7), except for two charnockites, which show very high Na_2O contents. The most basic charnockite (105775) has the lowest Na_2O content (1.49 wt.%) but also the highest CaO content (10.4 wt.%) (Table 6).

Most of the analyzed charnockites are hypersthene normative but have some olivine in the CIPW norm (2.8 to 8.7 wt.%), although xenolith U-3 has 15.8 wt.% normative quartz (Table 6). All have normative orthoclase (8–22 wt.%).

Trace elements

Charnockites show lower contents of REE-Y and HFSE (Th-U-Zr-Nb-Ta) than peraluminous granulite xenoliths, except the most felsic sample 105779. Moreover, they show slightly lower Rb-(Ba)-Cs contents, but similar Sr. More remarkable is their slightly lower Ni-(Cr)-V contents than felsic or pelitic xenoliths (Fig. 7).

According to REE and multi-element patterns the most basic charnockite 105775 is markedly different to the rest (Fig. 8a,b). It has the lowest trace-element contents and the flattest REE pattern, similar to those of some associated pyroxenite xenoliths. In fact, it has nearly the same multi-element pattern as websterite xenolith 102131 of Orejana *et al.* (2006), but has higher LILE contents (Rb, K, Sr, Ba). The other charnockites show a fractionated LREE pattern and a variably negative Eu anomaly, similar to those of the felsic granulite xenoliths, although with lower HREE contents (Fig. 8a). In normalised multi-element plots they show negative Th-U, Nb-Ta and Ti anomalies, and positive Pb and P anomalies. The lack of coherent element correlations suggests that the charnockite samples should not be treated as a single cogenetic group.

Sr-Nd-Pb isotopes

Measured Sr, Nd and Pb isotopic ratios for these xenoliths are given in Table 7. Their Sr-Nd isotope compositions

Table 6. Major (wt.%) and trace element (ppm) composition of the SCS pyroxene-bearing xenoliths.

Sample	**105775**	**103490-B**	**105779**	**U-3**	**103184**	**81845**	**105796**
	Charnockite	Charnockite	Charnockite	Charnockite	Opx-grt-granulite	Opx-grt-granulite	Opx-grt-granulite
SiO2	46.68	52.37	52.77	59.94	48.26	59.36	71.03
TiO2	0.78	1.26	0.49	0.60	1.66	1.12	0.60
Al2O3	18.08	19.32	18.98	13.98	19.55	17.29	13.75
Fe2O3	8.32	7.51	5.28	4.14	14.85	7.13	4.28
MnO	0.11	0.13	0.16	0.07	0.19	0.07	0.06
MgO	7.41	4.21	3.16	1.71	6.13	3.19	2.17
CaO	10.4	5.75	6.15	6.22	3.39	2.28	1.57
Na2O	1.49	4.61	5.26	3.17	2.49	3.15	3.37
K2O	1.65	1.38	2.59	3.38	0.93	3.89	1.62
P2O5	0.05	0.38	0.27	0.32	0.07	0.19	0.09
LOI	4.92	2.46	5.25	6.05	1.26	2.00	1.35
Total	99.89	99.38	100.36	99.58	98.79	99.67	99.89
ACNK*	0.78	0.99	0.84	0.69	1.74	1.28	1.35
Ba	312	329	2846	794	547	1050	703
Rb	119	46.1	99.6	119	13	121	50.1
Sr	257	409	1670	415	369	347	453
Pb	0.50	7.59	8.50	6.00	14.00	21.00	12.50
Th	0.10	2.92	7.16	0.24	5.27	37.90	2.38
U	0.03	0.88	3.56	0.25	1.05	1.43	0.38
Zr	34.5	367	146	121	137	263	157
Nb	2.11	11.80	8.84	6.00	13.60	7.70	3.47
Y	17.60	19.40	28.60	20.70	72.30	21.90	26.20
Sc	n.d.	n.d.	n.d.	11	37	17	n.d.
V	203	147	139	56	270	162	59
Co	32	25	27	8	27	21	9
Cr	636	161	102	16	172	100	69
Ni	50	58	86	15	37	47	19
Ga	17.40	24.20	24.40	16.00	24.00	22.00	14.80
Ta	0.11	0.67	1.41	0.32	0.62	0.50	0.20
Hf	1.26	8.40	4.47	3.20	3.90	7.20	3.98
Cs	4.81	3.37	0.59	3.00	4.70	7.70	2.70
La	3.35	22.10	33.40	19.70	35.70	62.60	37.60
Ce	7.89	48.30	64.30	43.00	67.10	127.00	62.80
Pr	1.34	6.17	8.04	5.30	7.60	15.00	6.71
Nd	7.45	25.70	32.70	22.10	29.30	56.00	24.20
Sm	2.74	5.27	6.95	5.09	7.20	8.34	4.13
Eu	0.78	1.62	1.23	1.39	2.62	2.46	2.11
Gd	3.13	4.57	6.02	5.31	9.95	5.31	4.22
Tb	0.53	0.65	0.94	0.87	2.00	0.76	0.72
Dy	3.19	3.57	5.31	4.44	12.80	4.11	4.49
Ho	0.64	0.69	1.02	0.81	2.74	0.84	0.91
Er	1.72	1.84	2.81	2.33	8.70	2.75	2.60
Tm	0.24	0.28	0.40	0.31	1.28	0.41	0.40
Yb	1.56	1.77	2.72	1.75	8.02	2.63	2.67
Lu	0.23	0.30	0.41	0.24	1.15	0.39	0.42
CIPW norm							
Q-	-	-	-	15.78	6.44	13.93	37.41
Or	10.36	8.48	16.19	21.46	5.72	23.71	9.76
Ab	13.36	40.48	39.83	28.76	21.87	27.44	29.02
An	40.02	27.34	21.65	14.91	17.06	10.51	7.46
C	-	0.61	-	-	8.75	4.27	3.85
Di	11.71	-	7.33	13.44	-	-	-
Hy	12.48	15.40	-	2.81	33.67	16.08	10.34
Ol	8.65	2.81	8.43	-	-	-	-
Ne	-	-	3.87	-	-	-	-
Mt	1.74	1.54	1.10	0.87	3.05	1.45	0.85
Ilm	1.57	2.40	0.98	1.23	3.29	2.19	1.16
Ap	0.12	0.86	0.62	0.75	0.16	0.43	0.20

n.d.: not determined. *ACNK = molar (Al_2O_3/(CaO+Na_2O+K_2O)).

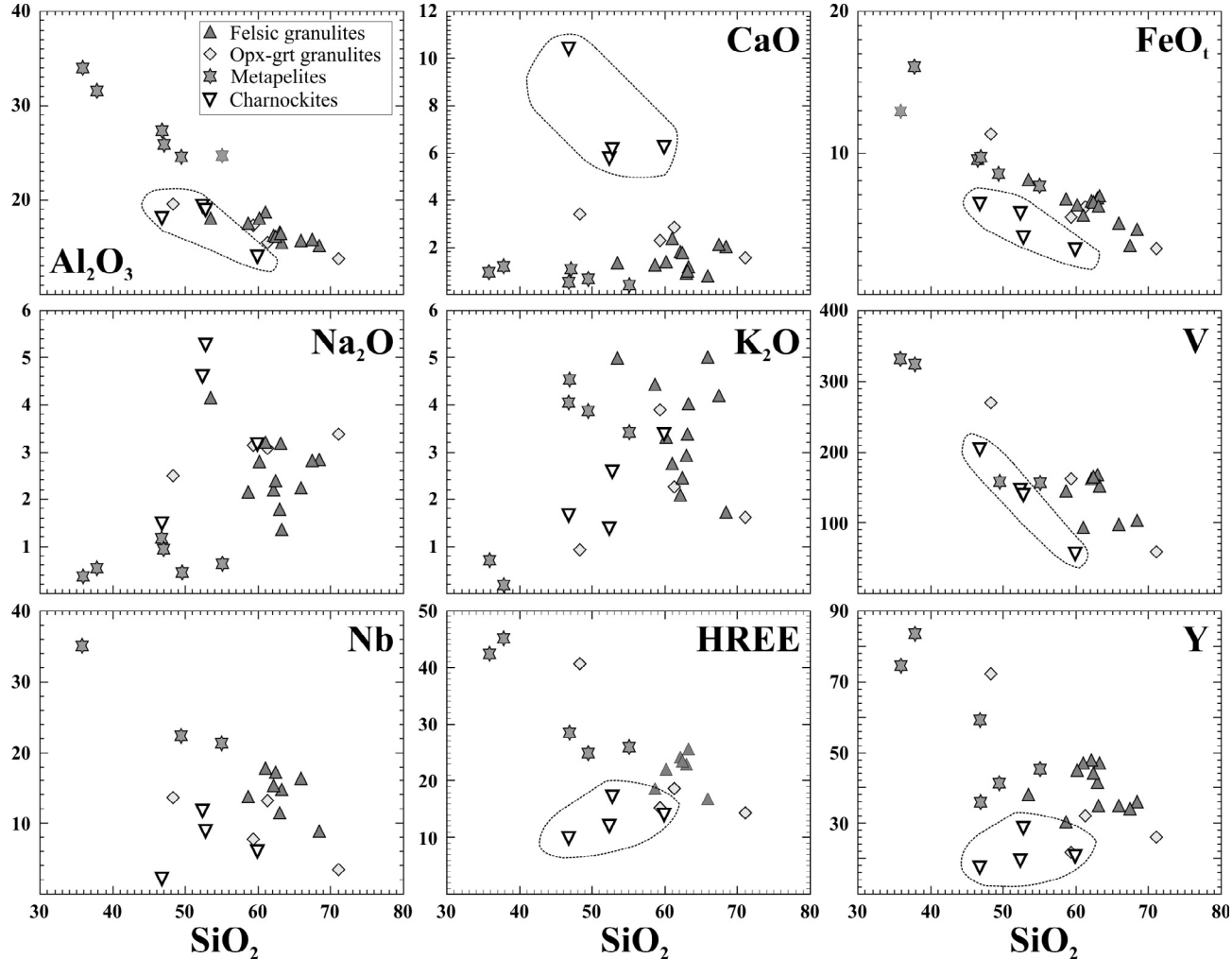

Fig. 7. Major (wt.%) and trace (ppm) elements *vs.* SiO_2 variation diagrams for SCS granulite xenoliths. Felsic and metapelitic xenoliths are taken from Villaseca *et al.* (1999).

are plotted in Fig. 9 together with isotopic values from the other granulite xenolith suites (Villaseca *et al.*, 1999) and from calc-alkaline pyroxenite xenoliths (Orejana *et al.*, 2006). Initial isotopic ratios have been calculated at 300 Ma, which is the average age for granulite recrystallization of the lower crustal xenoliths (Fernández Suárez *et al.*, 2006). In the age-corrected ε_{Nd} *vs.* $^{87}Sr/^{86}Sr$ diagram (Fig. 9), charnockites plot towards BSE values, and display a slightly lower Sr-Nd isotopic composition than associated peraluminous granulite xenoliths. Nevertheless, two of the most acid charnockites (U-3 and 103490B) plot inside the felsic granulite field. More basic charnockites have similar Sr and Nd isotope values to those pyroxenite xenoliths. The Pb isotope data confirms the similarity between the most basic charnockite 105775 and the calc-alkaline pyroxenite xenoliths, which yields the highest $^{206}Pb/^{204}Pb$ ratio (Fig. 10). Again, charnockite 103490B plots within the same Pb isotope compositional field as the other SCS granulite xenoliths (defined by felsic meta-igneous granulites, Table 7), although toward lower $^{208}Pb/^{204}Pb$ values (Fig. 10b).

The different SCS xenolith types show a restricted range in Pb isotope composition, similar to that defined by other European lower crustal xenoliths (Downes, 1993). The limited variation in initial Pb isotopic composition of SCS lower crustal xenoliths (charnockite, felsic and pelitic granulites) contrasts with their wide variation in ε_{Nd} and $^{87}Sr/^{86}Sr$ values.

Discussion

Nature of granulitic protoliths: restites or cumulates from previous magma underplating events?

Very scarce basic rocks are present in the SCS. Outcropping metamorphic rocks of Neoproterozoic to Lower Palaeozoic age are characterized by rare occurrences of meta-basites; minor continental-type tholeiitic meta-basites were described by Barbero & Villaseca (2000). The lack of basic magmatic input associated with the Hercynian collision is remarkable, estimated to be much less than

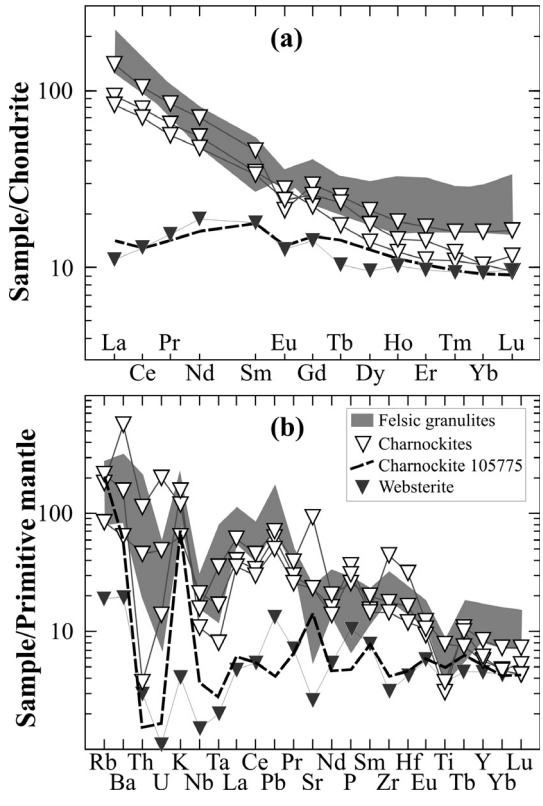

Fig. 8. Trace element diagrams for SCS granulite xenoliths: a) REE compositions normalised to chondrite values of Sun & McDonough (1989), b) incompatible trace element compositions normalised to primitive mantle values of McDonough & Sun (1995). Felsic granulite data from Villaseca *et al.* (1999), websterite data from Orejana *et al.* (2006).

1 vol.% of the total Hercynian SCS batholith (Villaseca *et al.*, 1998; Bea *et al.*, 1999; Villaseca & Herreros, 2000). The origin and nature of the protoliths of the basic to intermediate granulite xenoliths described in this work is relevant to clarify the composition and evolution of this complex orogenic continental sector.

The varied chemical composition of the charnockites suggests multiple origins. For example, the isotopic data point to different charnockite protoliths which cannot be related to a single petrogenetic process (*e.g.* a single layered igneous complex or a unique magmatic system, even involving assimilation of lower crustal rocks). Thus, the studied SCS charnockites reflect sampling of different granulite protoliths.

Some charnockite xenoliths could be recrystallized cumulates from previous Hercynian calc-alkaline magmatic events, subsequently fragmented at the base of the crust and included by the ascending Permian alkaline lamprophyres. This is based on the lack of hydrous minerals (amphibole or mica) and chemical similarities with the calc-alkaline ultramafic xenoliths. The clinopyroxene composition of charnockite 102131 is very similar to that of clinopyroxenes in the related websterite xenolith (Orejana *et al.*, 2006) (Fig. 5b and 6b). Charnockite orthopyroxene trace element contents are also within the same range shown by the accompanying websterite xenolith (Fig. 6a). Moreover, charnockite 105775 has a trace element whole-rock composition typical of a clinopyroxene-plagioclase cumulate, which resembles some pyroxenite xenoliths (Fig. 8). This charnockite also has the most Ca-rich plagioclase and its clinopyroxene displays a convex-upward chondrite-normalized REE pattern typical of clinopyroxene formed as deep cumulate crystals from basic magmas (Irving & Frey, 1984). Consequently, some charnockites may form part of a complex mafic-ultramafic sequence subsequently granulitized at the base of the crust after a magmatic underplating event. Their high-K content and Hy-normative character suggest a calc-alkaline affinity. In fact, their Sr-Nd isotopic composition plot within the range displayed by minor Hercynian calc-alkaline basic magmas, which outcrop as small scattered gabbroic bodies in the SCS (Bea *et al.*, 1999).

In contrast to the cumulate xenoliths discussed above, the lack of Ca-rich plagioclase and exsolution textures in pyroxenes, combined with a trace-element geochemistry that is not appropriate for plagioclase- or pyroxene-dominated cumulates (Berger *et al.*, 2005), suggest that most SCS charnockites are restitic rocks. The composition of restitic pyroxenes in melting experiments of various rocks (metapelites, metagreywackes, biotite-gneisses, basalts and tonalites) are shown in Fig. 5 and may furnish information on the charnockite protoliths. Thus, orthopyroxene formed by biotite breakdown (*e.g.* metapelites, gneisses) has higher Al_2O_3 contents than that orthopyroxene formed by hornblende breakdown in metaluminous protoliths (*e.g.* tonalites, basalts) (Fig. 5a). In a diagram of Al_2O_3 *vs.* CaO composition, orthopyroxene from metapelitic rocks plots towards the highest Al_2O_3 (and lowest CaO) contents; whereas those from meta-basalts have the highest CaO (and lowest Al_2O_3) contents. Charnockitic orthopyroxenes plot in an intermediate compositional field, which is closer to basic-intermediate (and metaluminous) protoliths, whereas garnet-bearing felsic granulites have orthopyroxenes of clear peraluminous felsic derivation (Al-rich graywackes or biotite-bearing gneisses) (Fig. 5a). Restitic orthopyroxene from dehydration-melting experiments in metaluminous tonalites (Singh & Johannes, 1996) match closely with the compositional field of charnockitic orthopyroxene.

Charnockite clinopyroxenes also plot in an intermediate field between restitic clinopyroxenes in melting experiments involving meta-tonalites (Singh & Johannes, 1996) and K-rich meta-basaltic andesites (not included in Fig. 5, sample YOS-55A from Sisson *et al.*, 2005). Restitic clinopyroxenes from more meta-basic protoliths (basalts or amphibolites) usually have higher Al_2O_3 contents (Springer & Seck, 1997; Sisson *et al.*, 2005) (Fig. 5b).

The absence of amphibole in metaluminous granulites is remarkable. Some dehydration melting experiments show that amphibole breakdown occurs below 900 to 950 °C (Beard & Lofgren, 1991; Patiño Douce & Beard, 1995; Skjerle & Johnston, 1996), suggesting that amphibole might be a stable restite phase during dehydration melting in the lower continental crust. Moreover, other melting ex-

Table 7. Sr, Nd and Pb isotope data for the SCS xenoliths.

Sample	105775	103490B	105779	U-3	103184	105796	95141*	95148*	77750*	U-42*	U-90*	102131**	104395**
Xenolith-type	*Charnock.*	*Charnock.*	*Charnock.*	*Charnock.*	*Opx-grt-granulite*	*Opx-grt-granulite*	*Felsic*	*Felsic*	*Metapelite*	*Metapelite*	*Metapelite*	*Websterite*	*Pyroxenite*
Rb (ppm)	119	46.1	99.64	119	13	50.15	97	85	108	148	126	10.5	7.6
Sr (ppm)	257.2	409	1670	415	369	453	186	240	141	151	233	47.2	60.7
$(^{87}Rb/^{86}Sr)$	1.34	0.33	0.17	0.83	0.10	0.32	1.51	1.03	2.22	2.84	1.57	0.64	0.36
$(^{87}Sr/^{86}Sr)m$	0.710342 ± 18	0.707974 ± 09	0.705821 ± 10	0.7095153 ± 07	0.711566 ± 07	0.707973 ± 23	0.716961 ± 10	0.716452 ± 10	0.726946 ± 10	0.721622 ± 06	0.72028 ± 03	0.707639 ± 05	0.706989 ± 06
$(^{87}Sr/^{86}Sr)_{300}$	0.70462	0.70658	0.70508	0.70597	0.71113	0.70661	0.71051	0.71207	0.71746	0.70951	0.71359	0.70489	0.70545
Sm (ppm)	2.73	5.27	6.95	5.09	7.20	4.13	6.25	8.13	11.80	9.45	6.97	2.7	3.4
Nd (ppm)	7.45	25.70	32.71	22.10	29.30	24.18	27.10	37.60	64.00	46.00	20.10	8.70	10.80
$(^{147}Sm/^{144}Nd)$	0.2215	0.1240	0.1284	0.1392	0.1485	0.1033	0.1396	0.1307	0.1120	0.1240	0.2101	0.1877	0.1886
$(^{143}Nd/^{144}Nd)m$	0.512641 ± 05	0.512362 ± 09	0.512285 ± 06	0.5123903 ± 04	0.512254 ± 03	0.512216 ± 05	0.512379 ± 08	0.512217 ± 07	0.511878 ± 03	0.511897 ± 03	0.512128 ± 07	0.512450 ± 03	0.512482 ± 03
$(^{143}Nd/^{144}Nd)_{300}$	0.512205	0.512119	0.512033	0.512117	0.511958	0.512013	0.512099	0.511960	0.511659	0.511653	0.511716	0.512081	0.512112
$E(Nd)_{300}$	−0.89	−2.60	−4.27	−2.63	−5.73	−4.66	−2.98	−5.69	−11.57	−11.69	−10.45	−3.33	−2.74
U (ppm)	0.03	0.88				0.38	0.39	0.83				0.09	0.07
Pb (ppm)	0.5	7.59				12.5	14	11	*Kfs.*	*Kfs.*	*Kfs.*	1.57	2.59
$(^{206}Pb/^{204}Pb)_{300}$	18.722	18.244				18.263	18.390	18.446	18.311	18.408	18.243	18.630	18.599
$(^{207}Pb/^{204}Pb)_{300}$	15.578	15.615				15.608	15.633	15.630	15.666	15.654	15.594	15.611	15.591
$(^{208}Pb/^{204}Pb)_{300}$	38.357	38.166				38.208	38.302	38.223	38.590	38.806	38.277	38.440	38.490

* Sr and Nd isotope data from Villaseca *et al.* (1999). ** Sr and Nd isotope data from Orejana *et al.* (2006). Uncertainties for the $^{87}Sr/^{86}Sr$ and $^{143}Nd/^{144}Nd$ ratios are 2 sigma errors in the last two digits.

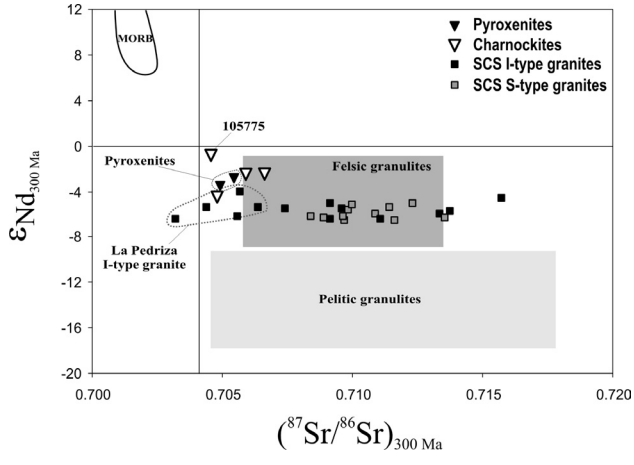

Fig. 9. Sr-Nd isotopic ratios at 300 Ma for the SCS granulite xenoliths. Field for calc-alkaline pyroxenite xenoliths from Orejana *et al.* (2006). Fields for felsic and pelitic granulite xenoliths from Villaseca *et al.* (1999), and for the SCS Hercynian granites from Villaseca *et al.* (1998). Also shown is unpublished compositional data for La Pedriza I-type granites.

periments on meta-basic rocks show amphibole to be stable above 975 °C (Hacker, 1990; Springer & Seck, 1997; Sisson *et al.*, 2005); its stability is a function of several factors including metamorphic conditions (P-T-oxygen fugacity) and whole-rock composition. The varied chemical composition of SCS charnockites and the presence of residual Ti-F-rich phlogopite in associated peraluminous granulite xenoliths suggest that amphibole was scarce or absent in the original pre-granulitic lithotypes, which would suggest long-term residence at lower crustal levels and recrystallization under high-T granulite facies conditions.

Pyroxene granulites and the SCS Hercynian granitoid plutonism

Sr-Nd-Pb isotope ratios and multi-element and REE patterns show that many SCS charnockites are similar in composition to associated peraluminous restitic felsic granulite xenoliths. The felsic composition of these charnockites, combined with their granoblastic texture and pyroxene compositions that are similar to those of restitic pyroxenes in melting experiments, suggests that most of the SCS pyroxene-bearing granulites could be residues left after extraction of a granitic melt. Villaseca *et al.* (1999) and Villaseca & Herreros (2000) suggested that the suite of garnet-bearing felsic granulite xenoliths represent residues left after extraction of granitic magma similar in composition to the peraluminous granitoids of the SCS batholith. The Hercynian age of zircon recrystallization obtained from some SCS granulite xenoliths is consistent with a genetic link to Hercynian granite magmatism (Fernández Suárez *et al.*, 2006). The more mafic and metaluminous composition of the studied charnockite xenoliths could link these granulites to the less peraluminous, I-type SCS granites. In fact, slightly peraluminous to subaluminous amphibole-bearing granites have been described in the region (Villaseca *et al.*, 1998; Villaseca & Herreros, 2000). Metaluminous restite is usually in equilibrium with moderately peraluminous melt in melting experiments (*e.g.* Patiño Douce & Beard, 1995; Sisson *et al.*, 2005).

Initial Sr-Nd isotopic ratios (at 300 Ma) of charnockite xenoliths (excluding the most basic, cumulate-like, 105775 sample) show a range of ε_{Nd} from −2.6 to −4.2 and $^{87}Sr/^{86}Sr$ from 0.7051 to 0.7066, values that only overlap slightly with the most isotopically primitive SCS granites (Fig. 9). Nevertheless, unpublished Sr-Nd data on SCS granites have recorded such unradiogenic Sr values in an I-type leucogranite pluton (La Pedriza massif) (Fig. 9). In addition, the granulite Pb isotope data presented in this work also corroborates the similarity between granulite xenoliths and outcropping Hercynian granites of I-type affinity. Figure 10 includes available Pb isotope data on SCS granites, mainly for the La Pedriza sector (Pérez-Soba, 1992), together with other Hercynian granites from central Spain (Los Pedroches batholith, S- and transitional-I-type granites; García de Madinabeitia, 2002). The granulite xenolith Pb isotopic data clearly match that of the Hercynian granite compositional field, thus reinforcing the

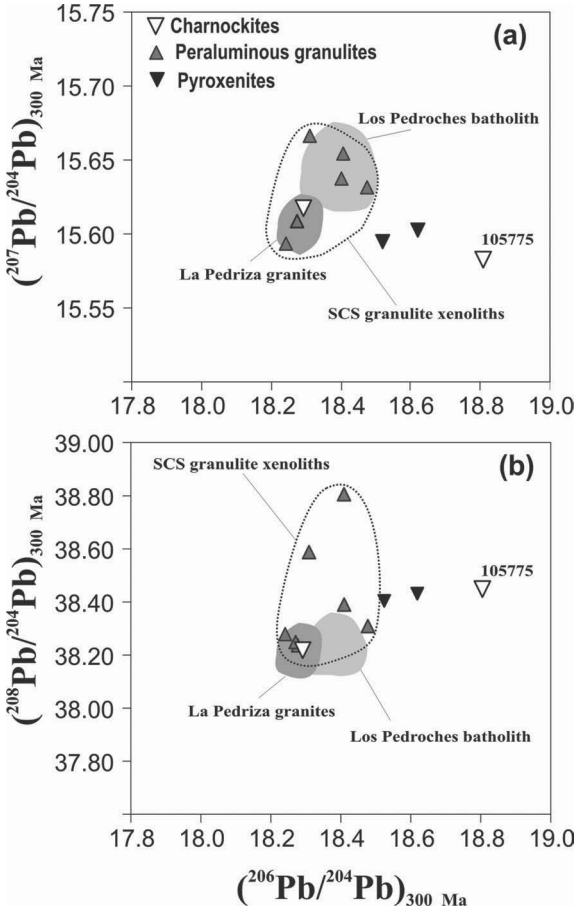

Fig. 10. Pb isotopic ratios at 300 Ma for the SCS granulite xenoliths and calc-alkaline pyroxenites: a) $^{207}Pb/^{204}Pb$ *vs.* $^{206}Pb/^{204}Pb$, b) $^{208}Pb/^{204}Pb$ *vs.* $^{206}Pb/^{204}Pb$. Also shown are fields for K-feldspars from Central-Iberian Hercynian granites: Los Pedroches batholith (García de Madinabeitia, 2002), La Pedriza sector (Pérez-Soba, 1992). Peraluminous granulites comprise felsic and metapelitic xenoliths.

granulite-granite connection in central Spain. A similar lower crustal derivation, based on Sr-Nd-Pb isotopic data, has been suggested for Hercynian granites of the French Massif Central (Downes *et al.*, 1997). Most of the granulite xenoliths with pelitic natures have different Sr-Nd isotopic ratios to the Hercynian granites from central Spain (Fig. 9 and 10) (Table 7), underlining their minor contribution to the SCS peraluminous granite batholith as has been previously stated (Villaseca *et al.*, 1998; 1999; Villaseca & Herreros, 2000).

Conclusions

SCS pyroxene-bearing xenoliths equilibrated at high $P-T$ conditions, mainly in the range of 900 to 1000 °C and 9 to 11 kbar. Although these ranges represent more extreme $P-T$ values, they overlap with estimates for the most abundant felsic granulites, indicating similar metamorphic conditions, and, therefore, they may have been sampled from the same depth in the lower crust.

The heterogeneity shown by SCS charnockite xenoliths implies contrasting origins. The most mafic samples could represent metamorphosed equivalents of mafic calc-alkaline magmas intruded at or near the crust-mantle boundary. Due to their spatial association with ultramafic pyroxenite xenoliths, they are interpreted as having crystallized initially as gabbroic cumulates, successively converted to granulites as they cooled. Nevertheless, the most abundant intermediate (SiO_2 > 52 wt.%) charnockite xenoliths could be restitic granulites after granite melt extraction; this is due to their appropriate pyroxene mineral chemistry and the strong overlap in initial Sr-Nd-Pb isotope ratios with outcropping Hercynian granites, mainly with those of I-type affinity.

If the abundances of mafic and felsic xenoliths in the SCS reflects the true abundance of these compositions in the lower crust, and if only a few of these mafic xenoliths are true cumulates from an underplating event at the crust-mantle boundary, then mantle-derived magmatism during Hercynian times in central Spain represents a minor episode of crustal accretion. This is in agreement with recent thermal modelling of the Hercynian collision by thickening of the central Iberian crust, if correct it would imply that granite magmatism does not require a significant addition of heat from mantle sources (Bea *et al.*, 2003).

Acknowledgements: We acknowledge the assistance of Alfredo Fernández Larios and José González del Tánago for the electron-microprobe analyses in the CAI of Microscopía Electrónica (UCM). We are grateful to Hilary Downes and Dan Lux for their constructive reviews, and to Angelo Peccerillo for the editorial handling. Laser mineral analyses were carried out at the Large Scale Geochemical Facility supported by the European Community Access to Research Infrastructure action of the Improving Human Potential Programme, contract number HPRI-CT-1999-00008. Pb isotope analyses have been also supported by the EU Access to Research Infrastructure action of the Improving Human Potential Programme during 2004 (Large Scale Geochemical Facility grant) and 2005 (SYNTHESYS grant under Framework Programme 6). This work is included in the objectives of, and supported by, the CGL-2004-02515 project of the Ministerio de Ciencia y Tecnología of Spain.

References

Al-Mishwat, A. & Nasir, S.J. (2004): Composition of the lower crust of the Arabian Plate: a xenolith perspective. *Lithos*, **72**, 54-72.

Barbero, L. & Villaseca, C. (2000): Eclogite facies relics in metabasites from the Sierra de Guadarrama (Spanish Central System): $P-T$ estimations and implications for the Hercynian evolution. *Min. Mag.*, **64**, 815-836.

Bea, F., Montero, P., Molina, J.F. (1999): Mafic precursors, peraluminous granitoids, and late lamprophyres in the Avila batholith; a model for the generation of Variscan batholiths in Iberia. *J. Geol.*, **107**, 399-419.

Bea, F., Montero, P., Zinger, T. (2003): The nature, origin, and thermal influence of the granite source layer of Central Iberia. *J. Geol.*, **111**, 579-595.

Beard, J.S. & Lofgren, G.E. (1991): Dehydration melting and water-saturated melting of basaltic and andesitic greenstones and amphibolites at 1, 3 and 6.9 kb. *Petrol.*, **32**, 365-401.

Berger, J., Féménias, O., Coussaert, N., Demaiffe, D. (2005): Magmatic garnet-bearing mafic xenoliths (Puy Beaunit, French Massif Central): P-T path from crystallisation to exhumation. *Eur. J. Mineral.*, **17**, 687-701.

Brey, G.P. & Kölher, T. (1990): Geothermobarometry in four phase lherzolites, part II: new thermobarometers, and practical assessment of existing thermobarometers. *J. Petrol.*, **31**, 1353-1378.

Brey, G.P., Nickel, K.G., Kogarko, L. (1986): Garnet-pyroxene equilibria in the system CaO-MgO-Al_2O_3-SiO_2 (CMAS): prospects for simplified ('T-independent') lherzolite barometry and an eclogite-barometer. *Contrib. Mineral. Petrol.*, **92**, 448-455.

Carignan, J., Hild, P., Mevelle, G., Morel, J., Yeghicheyan, D. (2001): Routine analyses of trace elements in geological samples using flow injection and low pressure on-line liquid chromatography coupled to ICP-MS; a study of geochemical reference materials BR, DR-N, UB-N, AN-G and GH. *Geostand. Newsl.,* **25**, 187-198.

Carrington, D.P. & Harley, S.L. (1995): Partial melting and phase relations in high-grade metapelites: an experimental petrogenetic grid inthe KFMASH system. *Contrib. Mineral. Petrol.*, **120**, 270-291.

Castro, A., Patiño-Douce, A., Corretgé, L.G., De la Rosa, J.D., El-Biad, M., El-Hmidi, H. (1999): Origin of peraluminous granites and granodiorites, Iberian Massif, Spain: an experimental test of granite petrogenesis. *Contrib. Mineral. Petrol.*, **135**, 255-276.

Condie, K.C., Cox, J., O'Reilly, S.Y., Griffin, W.L., Kerrich, R. (2004): Distribution of high field strength and rare elements in mantle and lower crustal xenoliths from the southwestern United States: the role of grain-boundary phases. *Geochim. Cosmochim. Acta*, **68**, 3919-3942.

Downes, H. (1993): The nature of the lower continental crust of Europe: petrological and geochemical evidence from xenoliths. *Phys. Earth Planet. Inter.*, **79**, 195-218.

Downes, H., Shaw, A., Williamson, B.J., Thirlwall, M.F. (1997): Sr, Nd and Pb isotopic evidence for the lower crustal origin of Hercynian granodiorites and monzogranites, Massif Central, France. *Chem. Geol.*, **136**, 99-122.

Dunn, A., Reynolds, P.H., Clarke, D.B., Ugidos, J.M. (1998): A comparison of the age and composition of the Shelburne dyke, Nova Scotia, and the Messejana dyke, Spain. *Canad. J. Earth Sci.*, **35**, 1110-1115.

Ellis, D. J. (1980): Osumilite-sapphirine-quartz granulites from Enderby Land, Antarctica: P-T conditions of metamorphism, implications for garnet-cordierite equilibria and the evolution of the deep crust. *Contrib. Mineral. Petrol.*, **74**, 201-210.

Fernández Suárez, J., Arenas, R., Jeffries, T.E., Whitehouse, M.J., Villaseca, C. (2006): A U-Pb geochronological study of zircons from a lower crustal xenolith of the Spanish Central System: a record of Iberian lithospheric evolution from Neoproterozoic to the Triassic. *J. Geol.*, **114**, 471-483.

García de Madinabeitia, S. (2002): Implementación y aplicación de los análisis isotópicos de Pb al estudio de las mineralizaciones y la geocronología del área Los Pedroches-Alcudia (Zona Centro-Ibérica). Ph D. Universidad del País Vasco, Bilbao, 217 p.

Hacker, B.R. (1990): Amphibolite-facies-to-granulite-facies reactions in experimentally deformed, unpowdered amphibolite. *Amer. Mineral.,* **75**, 1349-1361.

Harley, S.L. (1984): An experimental study of partitioning of Fe and Mg between garnet and orthopyroxene. *Contrib. Mineral. Petrol.*, **86**, 359-373.

Irving, A.J. & Frey, F.A. (1984): Trace element abundances in megacrysts and their host basalts; constraints on partition coefficients and megacrysts genesis. *Geochim. Cosmochim. Acta*, **48**, 1201-1221.

Kretz, R. (1983): Symbols for rock forming minerals. *Amer. Mineral.*, **68**, 277-279.

Le Maitre, R.W., Bateman, P., Dudek, A., Keller, J., Lameyre, J., Le Bas, M.J., Sabine, P.A., Schmid, R., Sorensen, H., Streickeisen, A., Wooley, A.R., Zannetin, B. (1989): A classification of igneous rocks and glossary of terms. Blackwell, Oxford, 193 p=p.

Loock, G., Stosh, H. G., Seck, H. A. (1990): Granulite facies lower crustal xenoliths from the Eifel, West Germany: petrological and geochemical aspects. *Contrib. Mineral. Petrol.*, **105**, 25-41.

McDonough, W.F. & Sun, S.S. (1995): The composition of the Earth. *Chem. Geol.*, **120**, 223-253.

Montel, J.M. & Vielzeuf, D. (1997): Partial melting of metagreywackes, part II. Compositions of minerals and melts. *Contrib. Mineral. Petrol.*, **128**, 176-196.

Moreno-Ventas, I., Rogers, G., Castro, A. (1995): The role of hybridization in the genesis of Hercynian granitoids in the Gredos Massif, Spain: inferences from Sr-Nd isotopes. *Contrib. Mineral. Petrol.*, **120**, 137-149.

Nair, R., & Chacko, T. (2002): Fluid-absent melting of high-grade semipelites: $P - T$ constraints on orthopyroxene formation and implications for granulite genesis. *J. Petrol.,* **43**, 2121-2142.

Newton, R.C. & Perkins, D.I. (1982): Thermodynamic calibration of geobarometers based on the assemblages garnet-plagioclase-orthopyroxene (clinopyroxene)-quartz. *Amer. Mineral.,* **67**, 203-222.

Nuez, J., Ubanell, A.G., Villaseca, C. (1982): Diques lamprofíricos norteados con facies brechoidales eruptivas en la región de La Paramera de Ávila (Sistema Central Español). *Cuad. Lab. Xeol. Laxe*, **3**, 53-73.

Orejana, D., Villaseca, C., Paterson, B.A. (2006): Geochemistry of pyroxenitic and hornblenditic xenoliths in alkaline lamprophyres from the Spanish Central System. *Lithos*, **86**, 167-196.

Patiño Douce, A.E. & Beard, J.M. (1995): Dehydration-melting of biotite gneiss and quartz amphibolite from 3 to 15 kbar. *J. Petrol.,* **36**, 707-738.

Patiño Douce, A.E. & McCarthy, T.C. (1998): Melting of crustal rocks during continental collision and subduction. In "When continents collide: Geodynamics and geochemistry of ultrahigh-pressure rocks" (B.R. Hacker and J.G. Liou, eds.). Kluwer Academic Publishers. 27-55.

Pérez-Soba, C. (1992): Petrología y geoquímica del macizo granítico de La Pedriza, Sistema Central Español. Ph D. Universidad Complutense, Madrid, 225 p.

Perini, G., Cebriá, J.M., López-Ruiz, J.M., Doblas, M. (2004): Permo-Carboniferous magmatism in the variscan belt of Spain and France: implications on mantle sources. *in*: "Permo-Carboniferous magmatism and rifting in Europe", M. Wilson, E.R. Neumann, G.R. Davies, M.J. Timmerman, M. Heeremans, B. Larsen, eds., Geol. Soc. London Spec. Publ. **223**, 415-438.

Pinarelli, L. & Rottura, A. (1995): Sr and Nd isotopic study and Rb-Sr geochronology of the Béjar granites, Iberian Massif, Spain. *Eur. J. Mineral.*, **7**, 577-589.

Pride, C. & Muecke, G.K. (1981): Rare earth element distributions among coexisting granulite facies minerals, Scourian Complex, NW Scotland. *Contrib. Mineral. Petrol.*, **76**, 463-471.

Reid, M.R. (1990): Ionprobe investigation of rare earth element distribution and partial melting of metasedimentary granulites. *in*: "Granulites and crustal evolution", D. Vielzeuf, Ph. Vidal, eds., Kluwer Acad. Publ., 507-522.

Reyes, J., Villaseca, C., Barbero, L., Quejido, A.J., Santos Zalduegui, J.F. (1997): Descripción de un método de separación de Rb, Sr, Sm y Nd en rocas silicatadas para estudios isotópicos. *Congr. Ibérico Geoquim.*, **I**, 46-55.

Rogers, N.W. & Hawkesworth, C.J. (1982): Proterozoic age and cumulate origin for granulite xenolith, Lesotho. *Nature*, **299**, 409-413.

Singh, J. & Johannes, W. (1996): Dehydration melting of tonalites. Part II. Compositions of melts and solids. *Contrib. Mineral. Petrol.*, **125**, 26-44.

Sisson, T.W., Ratajeski, K., Hankins, W.B., Glazner, A.F. (2005): Voluminous granitic magmas from common basaltic sources. *Contrib. Mineral. Petrol.*, **148**, 635-661.

Skjerlie, K.P. & Johnston, A.D. (1996): Vapour-absent melting from 10 to 20 kbar of crustal rocks that contain multiple hydrous phases: implications for anatexis in the deep to very deep continental crust and active continental margins. *J. Petrol.*, **37**, 661-691.

Soto, J.I. & Soto, V.M. (1995): PTMAFIC: software package for thermometry, barometry, and activity calculations in mafic rocks using an IBM-compatible computer. *Comput. Geoscie.*, **21**, 619-652.

Springer, W. & Seck, H.A. (1997): Partial fusion of basic granulites at 5 to 15 kbar: implications for the origin of TTG magmas. *Contrib. Mineral. Petrol.*, **127**, 30-45.

Storkey, A.C., Hermann, J., Hand, M., Buick, I.S. (2005): Using in-situ trace-element determinations to monitor partial-melting processes. *J. Petrol.*, **46**, 1283-1308.

Sun, S.S. & McDonough, W.F. (1989): Chemical and isotopic systematics of oceanic basalts; implications for mantle composition and processes. *Geol. Soc. London, Spec. Publ.*, **42**, 313-345.

Ulianov, A., Kalt, A., Pettke, T. (2006): Aluminous websterite and granulite xenoliths from the Chyulu Hills volcanic field, Kenya: gabbro-troctolitic cumulates subjected to lithospheric foundering. *Contrib. Mineral. Petrol.*, **152**, 459-483.

Upton, J., Aspen, P., Hinton, W. (2001): Pyroxenite and granulite xenoliths from beneath the Scottish Northern Highlands Terrane: evidence for lower-crust/upper-mantle relationships. *Contrib. Mineral. Petrol.*, **142**, 178-198.

Villaseca, C. & Herreros, V. (2000): A sustained felsic magmatic system: the Hercynian granitic batholith of the Spanish Central System. *Trans. R. Soc. Edinburgh: Earth Sci.*, **91**, 207-219.

Villaseca, C., Barbero, L., Rogers, G. (1998): Crustal origin of Hercynian peraluminous granitic batholiths of central Spain: petrological, geochemical and isotopic (Sr, Nd) constraints. *Lithos,* **43**, 55-79.

Villaseca, C., Downes, H., Pin, C., Barbero, L. (1999): Nature and composition of the lower continental crust in central Spain and the granulite-granite linkage: inferences from granulitic xenoliths. *J. Petrol.,* **40**, 1465-1496.

Villaseca, C., Martín Romera, C., De la Rosa, J., Barbero, L. (2003): Residence and redistribution of REE, Y, Zr, Th and U during granulite-facies metamorphism: behaviour of accessory and major phases in peraluminous granulites of central Spain. *Chem. Geol.*, **200**, 293-323.

Villaseca, C., Orejana, D., Pin, C., López García, J.A., Andonaegui, P. (2004): Le magmatisme basique hercynien et post-hercynien du Système Central Espagnol: essai de caractèrisation des sources manteliques. *C. R. Geosciences*, **336**, 877-888.

Villaseca, C., Orejana, D., Paterson, B.A. (2007): Zr-LREE rich minerals in residual peraluminous granulites, another factor in the origin of low Zr-LREE granitic melts? *Lithos* **96**, 375-381.

Watson, E.B., Wark, D.A, Thomas, J.B. (2006): Crystallization thermometers for zircon and rutile. *Contrib. Mineral. Petrol.,* **151**, 413-433.

Wells, P.R.A. (1977): Pyroxene thermometry in simple and complex systems. *Contrib. Mineral. Petrol.,* **62**, 129-139.

Witt-Eickschen, G. & Seck, H.A. (1991): Solubility of Ca and Al in orthopyroxene from spinel peridotite: an improved version of an empirical geothermometer. *Contrib. Mineral. Petrol.,* **106**, 431-439.

Wood, B. J. & Banno, S. (1973): Garnet-orthopyroxene and garnet-clinopyroxene relationships in simple and complex systems. *Contrib. Mineral. Petrol.*, **42**, 109-124.

Zack, T., Moraes, R., Kronz, A. (2004): Temperature dependence of Zr in rutile: empirical calibration of a rutile thermometer. *Contrib. Mineral. Petrol.,* **148**, 471-488.

Received 19 October 2006
Modified version received 12 April 2007
Accepted 7 Mai 2007